

Why may consider rainfall space-time variability in Precision Agriculture?

Felipe Gustavo Pilau (✉ fgpilau@usp.br)

University of São Paulo

Thais Letícia Santos

University of São Paulo

Rafael Battisti

Federal University of Goiás

Klaus Reichardt

University of São Paulo

Ivo Zution Gonçalves

University of Nebraska-Lincoln, Daugherty Water for Food Global Institute. Lincoln

Research Article

Keywords: rainfall, precision agriculture, Glycine max L., crop modeling

Posted Date: April 21st, 2023

DOI: <https://doi.org/10.21203/rs.3.rs-2827581/v1>

License:   This work is licensed under a Creative Commons Attribution 4.0 International License.

[Read Full License](#)

Abstract

Brazil is one of the largest soybean producers in the world, however, there are still yield gaps in crops, mainly linked to weather conditions. Based on it, this paper quantifies the spatial variability of rainfall based on two dense networks of rain gauges and analyzes the influence on the attainable productivity (Y_a) of the soybean crop. The study was carried out in Piracicaba, SP. For the first rain gauge network a measuring campaign was conducted from 1993 to 1994, with 10 gauges distributed in 1,000.0 ha. The second rain gauge network measuring campaign was conducted from 2016 to 2018, with 9 gauges sampling 36.0 ha. To evaluate the influence of rainfall spatial variability on soybean yield a multi-model (FAO, DSSAT, and MONICA) simulation was used. The relative production loss ($Y_{g_{rel}}$) caused by water deficiency was simulated for 3 sowing dates and each rainfall sampling point. The results showed that the spatial variability of precipitation has a direct influence on attainable productivity (Y_a). However, the magnitude of rainfall variability is not directly replicated in yield. The temporal variability, between the different sowing times, had a major influence on soybean yield.

1. Introduction

Brazilian farmers who adopt precision agriculture often map crop yield in their crops, which has revealed variability in most areas (Amado et al. 2007; Mattioni et al. 2011; Bottega et al. 2017). The spatial variability of agricultural production results from complex interactions between factors. Despite the increasing adoption of techniques that allow the study of chemical, physical (Faraco et al. 2008; Mattioni et al. 2013; Dalchiavon et al. 2017), biological and microbiological distinctions of the soil (Lamb and Brown 2001; Monquero et al. 2008) of production areas, correctable for productivity variability, the analysis of meteorological elements, especially precipitation, is still little studied (Mesas-Carrascosa et al. 2015; Keswani et al. 2019).

To determine the temporal and spatial variability of precipitation, meteorological radars are used. Lenzi et al. (1990), Venäläinen and Heikinheimo (2002), and Gleason et al. (2008) are studies that highlight the high space-time resolution of the data, with the ability to locate areas of rain in almost real-time, with emphasis on those caused by small-scale convective systems, which are among the most elusive phenomena for weather station networks. In Brazil, however, due to the unavailability of data, the agricultural use of meteorological radar data is still limited.

As an alternative to weather radars, there are satellite products, such as TRMM (Huffman et al. 2007), CHIRPS (Funk et al. 2015), GPM (Huffman et al. 2019), GSMaP (Mega et al. 2014), PERSIANN (Ashouri et al. 2015), among others, suitable for analyzing the space-time variability of precipitation, even if the spatial resolution is greater than $0.05^\circ \times 0.05^\circ$ (Mashingia et al. 2014). Such kind of data can be combined with other data and models, which make it possible to identify the productive potential of crops, emerging as an opportunity to overcome the challenges of spatial and temporal dimensioning and, therefore, improve the understanding of yield gaps of crops (Lobell 2013).

Despite these meteorological information sources, not always being available or ready to use, the allocation of pluviometer meshes in agricultural properties in Brazil is not uncommon. This is the method often used by farmers to quantify precipitation and identify the presence of time-space variability in their crops. The adoption of this type of meteorological monitoring is increasing, not only in Brazil, due to the expansion of methods that also provide connectivity to rural areas, and the increase in the supply of sensors, such as meteorological stations/web platforms/APPs (Pierce and Elliott 2008; Jayaraman et al. 2016).

Regarding the results originating from pluviometric grids carried out in Brazil (Reichardt et al. 1995; Camargo and Hubbard 1999; Bega et al. 2005, Camargo et al. 2005; Chierice and Landim 2014; Almeida et al. 2016; Siciliano et al. 2018; Souza and Nascimento, 2020) and several other countries (Stol 1972; Schilling 1991; Graef and Haigis 2001; Krajewski et al. 2003; Jensen and Pedersen 2005; Pedersen et al. 2010; Gires et al. 2014; Tokay et al. 2014), it highlighted the ability to detect the temporal and spatial variability of precipitation, which increases with the predominance of convective systems, and that environmental characteristics such as orography, vegetation, watersheds or the presence of water bodies contribute to the irregularity.

Rainfall measurements made by precipitation networks, at the farm level improve information for the analysis of yield gaps in the crop fields (O'Neal et al. 2002; Lobell 2013; Lobell et al. 2015) if combined with crop models (Boote et al. 1998, 2003; Robertson and Camberly 1998; Jones et al. 2003; Nendel et al. 2011) can enhance the understanding of production variability, allowing to separate the causes into meteorological and management factors.

The general objective of the article was to carry out an agrometeorological analysis focusing on precipitation time-space variability. The specific objectives were (i) to characterize the variability of precipitation measured by two pluviometry grids, with domain areas of 1,000.0 ha and 36.0 ha, and (ii) to characterize how plant growth models can be used to identify the spatial variability of soybean yield as a function of the variability of precipitation measured by pluviometry grids.

2. Material And Methods

2.1 Experimental area

To quantify the variability of precipitation, data from two pluviometry grids were used. The first rainfall grid (MP1) was installed by Reichardt et al. (1995) in 1993, to measure daily rainfall variability on a local scale of 1,000.0 ha. The second pluviometer grid (MP2) was installed in 2016 to quantify the variability of precipitation in a smaller area of 36.0 hectares (Fig. 1). The pluviometry grids MP1 and MP2 were located in the municipality of Piracicaba, state of São Paulo, Brazil, in an area belonging to the College of Agriculture "Luiz de Queiroz", University of São Paulo (ESALQ/USP).

The climate in the region is classified as Cwa (Köppen classification) humid tropical, with rains concentrated between October and March and a dry period in autumn-winter (Alvares et al. 2013).

According to historical data, annual precipitation is $1350 \text{ mm year}^{-1}$.

For MP1, based on the description of the installation locations of the pluviometers (Reichardt et al. 1995), their geographic positioning was determined. When installing the MP2 grid rain gauges, the geographic position of each equipment was marked with GNSS signal receivers (Garmin, model GPSMap 62s). The same equipment was used to demarcate the MP1 coordinates. All data have geographic coordinates and UTM-type plane-rectangular coordinates (UTM projection), having the WGS 84 system, zone 23S, as a spatial reference.

2.2 Precipitation measurement

The nine pluviometers that formed the pluviometry grid MP1 (Reichardt et al. 1995) were randomly distributed in the ESALQ/USP area. The shortest distance between the measurement points was 640 m, while the longest was 4406 m apart.

Measurements were taken between November 1993 and October 1994, on a daily scale, adding up to 364 days of rainfall records. The equipment was manual, with a collection area of 300 cm^2 and a measurement accuracy of 0.1 mm. The rain gauges were installed 1.5 m above the ground surface, leveled, and free of obstacles in a circle of at least 20 m in radius. A tenth collection point was the pluviometer at the ESALQ/USP weather station (Fig. 1).

In the experimental area of ESALQ/USP, called "Fazenda Areão", the second pluviometry grid (MP2) was installed. Nine rain gauges were distributed at a distance of approximately 200 m from each other, except P7 (Fig. 1), in the shape of a square grid (Fig. 1). For this grid, data were collected from November 8, 2016, to January 22, 2018. A tenth rain gauge was also installed at the ESALQ/USP weather station, 2250 m from the center of MP2. The minimum and maximum spacing between pairs of MP2 rain gauges were 157 m and 612 m, respectively.

The MP2 rain gauges were of the "tipping bucket" model (Vaisala), with a collection surface of 380 cm^2 . The equipment, previously calibrated, was installed 1.5 m above the surface, leveled, and connected to data acquisition systems (Log Chart II), storing measurements every minute.

2.3 Precipitation data analysis

The series of precipitation data from MP1 (Reichardt et al. 1995) and MP2 were evaluated to identify erroneous data and measurement failures. As the grids were composed of nine pluviometers, in addition to the pluviometers installed at the Weather Station of ESALQ/USP (MP1 and MP2), it was possible to estimate the uncertainty of the measurements of each instrument from the deviations of the average obtained from the pluviometers in operation. A validation method was also applied to identify erroneous data (Estévez et al. 2011). The analysis was based on the consistency test called the "range test" (Eq. 1).

$$0 \leq P \leq P_{\text{MAX}} \quad (1)$$

where P is the daily precipitation (mm) measured by each rain gauge and P_{MAX} is the maximum daily precipitation value from historical data for Piracicaba, SP.

2.4 Soybean Yield Models and Simulation

To reduce the uncertainties in the simulations, the set of models' approaches was used (Asseng et al. 2013; Martre et al. 2015), recently validated for the soybean crop in several regions of Brazil (Battisti et al. 2017). Thus, based on the FAO models – Agroecological Zone (Doorenbos and Kassam 1979), the Model for nitrogen and carbon in agro-ecosystems v. 2.11 (Nendel et al. 2011) called MONICA and the CropSystem Model – CROPGRO – Soybean v. 4.6.1 present in the Decision Support System for Agrotechnology Transfer platform (Boote et al. 1998, 2003; Jones et al. 2003) called DSSAT, previously calibrated and validated for the region of Piracicaba, SP (Battisti et al. 2017), potential yield (PP , kg ha^{-1}), attainable yield (PA , kg ha^{-1}) and relative yield loss (Yg , in %) were estimated (Eq. 2).

$$Yg = \left(1 - \frac{PA}{PP}\right) 100$$

2

The multi-model set was then obtained from the arithmetic mean of the yields simulated by the three models.

For the pluviometric meshes (MP1 and MP2) the simulations used the three segments of precipitation data of each pluviometric mesh, with 130, 120 and 110 days counted from the sowing dates: November 15, December 15 and January 15 following the recommendation of the Climatic Risk Zoning for Soybean Crop (MAPA 2020). Thus, simulations for each of the three sowing dates were processed for each precipitation sample point in the grids (Fig. 1), incorporating precipitation variability.

All other meteorological elements required as input data by the models used were obtained from the weather station of ESALQ/USP and considered uniform for all simulation points.

The simulations aimed to evaluate the potential (PP) and attainable (PA) yield of a GMR 6.5 cultivar, like the cv. BRS 284 that was used to calibrate the models tested by Battisti et al. (2017).

From an undisturbed soil sample, collected at point (P4) of MP2, the soil water retention curve was obtained (van Genuchten 1980). Assuming soil homogeneity within the areas of MP1 and MP2, to analyze only the effect of precipitation on productivity, based on moisture at field capacity (θ_{cc}), of $0.338 \text{ cm}^3 \text{ cm}^{-3}$ and at wilting point (θ_{pmp}) of $0.249 \text{ cm}^3 \text{ cm}^{-3}$, and the maximum depth of the root system (z) of 0.85 m, the maximum soil water storage capacity (CAD) (Eq. 3) of 75 mm was obtained.

$$CAD = (\theta_{cc} - \theta_{pmp}) z$$

3

3. Results And Discussion

From each series of precipitation data and pluviometry grids MP1 and MP2, the three segments of precipitation data were separated, respectively with 130, 120, and 110 days of measurements, starting on November 15, 1993 (MP1) or 2016 (MP2), December 15, 1993 (MP1) or 2016 (MP2) and January 15, 1994 (MP1) or 2017 (MP2), to analyze the variability of precipitation in periods recommended for soybean production in Piracicaba, SP, Brazil (Figs. 2 and 3).

Regarding MP1, in the first series of data (11/15/93 to 03/24/1994) 46 rainy days were recorded, 20 days with at least 10.0 mm day^{-1} [Figure 2(2a)]. The average volume accumulated over the 130 days was 634.6 mm. Analyzing the precipitation of each of the MP1 rain gauges, during these 130 days, an average standard deviation for the cycle of 3.77 mm day^{-1} was obtained, with a maximum value of 13.5 mm day^{-1} . When analyzing the accumulated precipitation at each point of the sampling grid, and again quantifying the differences between points, a temporal increase in the standard deviation is observed, which at the end of the cycle reached 22.3 mm, a value close to 5% of the water demand from soybean cultivation in the study region (Oliveira 2018).

During the second analyzed series of MP1, from 12/15/1993 to 04/13/1994, 42 days with precipitation were recorded, 4 days less than the first season, considering that in this case, the series had 10 days less [Figure 2(2a)]. Considering this total, in 18 days the accumulated precipitation was at least 10 mm day^{-1} . The average accumulated precipitation in this second series was 597.3 mm, 37.3 mm less than in the first series. Over the 120 days evaluated, the mean standard deviation was 3.6 mm day^{-1} . The maximum standard deviation was 13.5 mm day^{-1} , on February 9, 1994, when the precipitation was 19.3 mm day^{-1} , considering a minimum of 1.3 mm day^{-1} (P9) and a maximum of 31.8 mm day^{-1} (P6). Still regarding the differences between the measurement points of MP1, at the end of the second series analyzed (120 days) the standard deviation concerning the data from the nine rain gauges was 24.0 mm, very close to that recorded for the first series [Figure 2(1a)].

The third series of MP1 precipitation data, with 110 days measured from January 15, 1994 [Figure 2(3a)], accounted for 40 rainy days, with 15 days having accumulated precipitation of at least 10 mm day^{-1} . The average accumulated precipitation in the nine pluviometers of the MP1 grid was 544.8 mm, respectively 14.2% and 8.8% less than in the first [Figure 2(1a)] and second [Figure 2(2a)] series, highlighting the temporal differences between the three series. Regarding the variation between measurement points over the 110 days, the mean standard deviation for the cycle was 4.0 mm day^{-1} , with a maximum coefficient of variation of 13.5 mm day^{-1} . Temporally, the standard deviation of the accumulated at each point, in the 110 days of measurement, was 29.7 mm, confirming the variability and a possible implication in the simulated soybean yield for each measurement point.

Regarding the data collected from the pluviometry grid MP2, for each series (Fig. 3) the variability of precipitation was also characterized for periods coinciding with soybean production in Piracicaba/SP, pointing to a difference in distribution, with prominence for differences between grades.

In the first series of MP2, of 130 days (11/15/2016 to 03/14/2017), 80 rainy days were recorded, 27 days with at least 10 mm day^{-1} [Figure 3(1a)]. The total accumulated volume was 708.7 mm. Evaluating the precipitation data for the 130 days, it was found that the mean grid standard deviation was 1.1 mm day^{-1} . Even the maximum standard deviation value was low, 4.3 mm day^{-1} . When analyzing the accumulated precipitation in each pluviometer and again quantifying the differences between points, a temporal increase in the standard deviation is observed, which at the end of this series of 130 days was 26.6 mm [Figure 3(1a)].

As for the second series [Figure 3(2a)], of 120 consecutive days from 12/15/2016, there were 68 rainy days, 12 days less than during the first series of MP2 [Figure 3(1a)], with 25 days of accumulated rain equal to or greater than 10 mm day^{-1} . The average precipitation accumulated by the grid, during the 120 days, was 669.8 mm, 38.9 mm less than in the first series [Figure 3(1a)], this one with 130 days. Regarding differences between rain gauges, the mean standard deviation for the 120 days was 1.2 mm day^{-1} . The maximum standard deviation value of this second MP2 data series was 8.1 mm day^{-1} , recorded on April 6, 2017, when the average precipitation accumulated by the grid was 79.3 mm day^{-1} , twice as much against the maximum standard deviation recorded for the first series [Figure 3(1a)]. At the end of the 120 days of measurements, the standard deviation for accumulated precipitation reached 31.4 mm, surpassing the temporal difference of the first series [Figure 3(1a)], once again indicating the probability of having spatial variability in the yield motivated by a meteorological element, in the case of precipitation.

Although the difference between the averages accumulated precipitation between the first two analyzed series of MP2 (Fig. 3(1a) and 3(2a)) was small, 5.5%, the temporal distributions naturally showed to be different, characterizing how different the meteorological influence can be on the production carried out at different times of the year, even in the same area.

Over the 110 days of the third analyzed series of MP2 [Figure 3(3a)], from January 15 to May 4, 1994, 53 rainy days were recorded, 21 days with at least 10 mm day^{-1} accumulated. At 110 days, the average precipitation accumulated by the nine pluviometers of the MP2 grid was 549.4mm, respectively 22.4% and 18.0% less than in the first [Figure 3(1a)] and second [Figure 3(2a)] series. Regarding the differences in measurement between rain gauges over the 110 days, the mean standard deviation for the cycle was 1.38 mm day^{-1} , with a maximum value of 8.0 mm day^{-1} . Temporally, the standard deviation concerning the accumulated at each point in the 110 days of measurement was 24.9 mm [Figure 3(3a)].

The reductions in accumulated precipitation from the first to the third series (5.9% from the first to the second and 14.1% from the first to the third) of grid MP1 (Fig. 2) were lower than the reductions of 7.7% (130 to 120 days) and 15.4% (130 to 110 days) over time. Similarly, analyzing data from MP2, a reduction of 5.5% in accumulated precipitation was verified between the first (130 days) and second (120 days) series (Fig. 3), once again smaller than the reduction over time. However, for this pluviometry grid, the reduction in accumulated precipitation, by 22.5% from the first to the third (110 days) series, was proportionally greater than the reduction over time between the referred series.

Battisti (2016), when presenting results for successive soybean sowing dates for Piracicaba (SP), defines that there is a reduction in yield potential to sowing delay, due to water deficiency. The results (Figs. 2 and 3), which mostly did not characterize a reduction in accumulated precipitation proportionally to the time of the analyzed data series, may result in deficiency since the energetic condition determines differences in crop evapotranspiration that extrapolate the temporal differences (Figs. 4 and 5). Furthermore, the differences observed between the measurement points of each of the grids (Figs. 2 and 3), reflecting differences in time, would most likely cause productive differences between the points.

In addition to precipitation, air temperature and global solar radiation (Q_g) were also evaluated for the series related to the soybean production period (Figs. 4 and 5). However, unlike precipitation, measured individually at each of the nine points of MP1 (Fig. 2) and MP2 (Fig. 3), these two meteorological elements did not have their variability quantified within the grids, having only daily data for each grid (Figs. 4 and 5).

The average air temperature showed little variation between the three series of data related to theoretical cycles of soybean production (Figs. 4 and 5). From MP1, in the first series, the average temperature was 24.2°C , with a slight tendency to decrease over time (Fig. 4A). For the second series of the same grid a thermal condition very similar to the first (Fig. 4A), with an average temperature of 24.5°C , and a trend of thermal decrease (Fig. 4B), being on this occasion higher than that registered for the first series. In the third series (Fig. 4C), despite the average temperature of 24.3°C , once again being close to that of the two previous series (Figs. 4A and 4B), the delay in sowing ends up subjecting the crop to a thermal decrease more intense ($-0.04^{\circ}\text{C day}^{-1}$).

Global solar radiation, which plays a key role in plant growth and development, also showed different cumulative values throughout each series. Regarding the MP1 data, in the first series the accumulated solar radiation was $2,177.3 \text{ MJ m}^{-2}$ (Fig. 4A) in the second $2,058.6 \text{ MJ m}^{-2}$ (Fig. 4B) and in the third $1,952.4 \text{ MJ m}^{-2}$ (Fig. 4C). The difference from one cycle to the other was approximately 5%, and from the first to the third, the radiant energy reduction was 10.33%.

For MP2, the average air temperature in the first series was 24.2°C (Fig. 5A), with a positive trend throughout the cycle, unlike the second (Fig. 5B) and third (Fig. 5C) series, both with a trend of temporal reduction of the average air temperature, which presented average values of 24.1°C and 23.0°C .

Regarding MP2, the global solar radiation accumulated in the first (Fig. 5A) and second (Fig. 5B) series were similar, reaching $2,573.3$ and $2,502.1 \text{ MJ m}^{-2}$, respectively. In the third series (Fig. 5C), despite the lower precipitation volume [Figure 3(3a)] and, therefore, probably a longer period of clear sky, the reduction of the photoperiod and consequently the availability of radiant energy (SR) resulted in $2,233.1 \text{ MJ m}^{-2}$ accumulated, an average of 12% less energy radiant compared to the two previous series.

The average temperature values of the three series, the MP1 (Fig. 4) and MP2 (Fig. 5) grids are favorable to the growth and development of the soybean crop (Farias et al., 2007). Critical temperatures were also

not observed which, below or above them, could affect the growth and development of soybeans.

The reduction of accumulated global solar radiation due to delayed sowing and the reduction of the development cycle may result in a reduction in the yield potential of the soybean crop (PP). Zanon et al. (2016) describe, for Rio Grande do Sul state, Brazil, that the delay in soybean sowing exposes the plants to reduced air temperature and solar radiation (Figs. 4 and 5), especially during reproductive stages, which explains the yield loss of $26 \text{ kg ha}^{-1} \text{ day}^{-1}$ for crops sown from November 4, considering crops without water limitation.

Based on the set of models, as recommended by Asseng et al. (2013) and Martre et al. (2015), estimated potential yield (PP, kg ha^{-1}), attainable yield (PA, kg ha^{-1}), and relative yield loss (Yg, %) for areas of 1,000.0 ha (MP1) and 36.0 ha (MP2) were obtained (Tables 1 and 2). The simulations, carried out individually for each of the nine precipitation measurement points in the MP1 and MP2 grids (Fig. 1), aimed to isolate the effect of precipitation variability on soybean PA and Yg. Therefore, the soil of the two areas was considered homogeneous in terms of water storage capacity, a factor that would affect the simulations, reducing or increasing the deviations between yield data regardless of precipitation.

Regarding MP1, as the simulations did not consider the spatial variability of air temperature and global solar radiation (Fig. 4), using the same set of daily data for all nine points (Fig. 1), PP was variable only between sowing dates. The simulation performed for the sowing date of November 15, 1993, resulted in a PP of $5,654.3 \text{ kg ha}^{-1}$. The results also showed a reduction in PP with the delay in soybean sowing, with $5,320.0 \text{ kg ha}^{-1}$ and $4,594.3 \text{ kg ha}^{-1}$ for the simulations started on December 15, 1993, and January 15, 1994, respectively.

It should be noted that the delay in sowing and consequent reductions in cycle lengths led to a decrease in the availability of radiant energy (Fig. 4), the main cause of the decrease in PP (Battisti et al. 2013). The PP values are similar to the PP values described by Battisti (2016) and Silva (2018) for Piracicaba (SP), for the same sowing period.

For MP1, the PA (Table 1), conditioned to water availability, reflected the variability of precipitation among the nine measurement points of MP1 (Fig. 2) in the three series. PA data for simulated sowing on November 15, 1993 point to an average of $3,951.2 \text{ kg ha}^{-1}$, with a standard deviation of 132.8 kg ha^{-1} . Similar PA variability was observed for the other two sowing dates, when the average PA was $4,005.9 (\pm 160.8) \text{ kg ha}^{-1}$ for December 15, 1993, and $3,261.5 (\pm 127.6) \text{ kg ha}^{-1}$ for January 15, 1994.

Table 1

Accumulated precipitation (AC, mm), attainable yield (PA), and relative yield loss (Yg) simulated for soybean, for each point of the pluviometry grid MP1. Theoretical sowing dates: November 15, 1993, December 15, 1993, and January 15, 1994. Grouping results of the FAO – Agroecological Zone, MONICA, and DSSAT models.

Point	Nov 15, 1993			Dec 15, 1993			Jan 15, 1994		
	AC (mm)	PA (Kg ha ⁻¹)	Yg (%)	AC. (mm)	PA (Kg ha ⁻¹)	Yg (%)	AC (mm)	PA (Kg ha ⁻¹)	Yg (%)
P1	605.2	3752.2	33.6	583.4	3927.0	26.2	534.9	3250.5	29.2
P2	628.1	4101.9	27.5	566.1	4151.5	22.0	495.4	3277.2	28.7
P3	616.1	3951.6	30.1	595.8	3982.9	25.1	564.1	3372.4	26.6
P4	623.9	3908.9	30.9	571.6	3846.3	27.7	525.0	3036.1	33.9
P5	660.3	4000.3	29.3	599.4	3924.3	26.2	532.8	3180.6	30.8
P6	645.6	4067.3	28.1	615.4	4076.1	23.4	571.7	3324.3	27.6
P7	645.8	4006.5	29.1	617.1	4048.6	23.9	554.3	3208.8	30.2
P8	671.0	4043.0	28.5	641.2	4309.6	19.0	595.7	3488.4	24.1
P9	615.3	3728.7	34.1	585.8	3787.2	28.8	529.5	3215.6	30.0
Mean	634.6	3951.2	30.1	597.3	4005.9	24.7	544.8	3261.5	29.0
SD	22.3	132.8	2.3	24.0	160.8	3.0	29.8	127.6	2.8
CV	3.5	3.4	7.8	4.0	4.0	12.2	5.5	3.9	9.6

SD is the standard variation; CV is the coefficient of variation (%).

The average attainable yield obtained for the December 15, 1993 sowing was higher for earlier sowings, even with a lower cycle and potential yield (Table 1). It turns out that the water condition, due to the temporal distribution of precipitation (Fig. 2), coinciding with the stages of reproductive development, was better in this second series.

In the simulated cycle from November 15, 1993, the average relative yield loss (Yg) was 30.1%, with a standard deviation of 2.3% to the nine sample points of MP1 (Table 1). In this first series, the mean precipitation was 634.6mm, with a standard deviation of 22.3mm (Table 1). In this case, using the results of the coefficient of variation, it is observed that the achievable yield variability, based on the coefficient of variation of 3.4%, reflected the variability of precipitation, which had a CV of 3.5%.

The simulated yield losses (Yg) for the third (latest) production cycle of MP1 were intermediate to the first two, with averages of 29% (Table 1). Despite the standard deviation of precipitation (29.8 mm) and CV (5.5%) being greater than those observed for the first two production cycles (Fig. 2), the coefficient of

variation of PA (3.9%), was not the highest (Table 1). This result reiterates that there is no direct relationship between accumulated precipitation and PA for a production cycle, because even with greater variability, the effects of a dry period depend on the phenological stage of the crop, with greater or lesser influence depending on the plant susceptibility to water stress.

Table 2

Accumulated precipitation (mm), attainable yield (PA), and relative yield loss (Yg) simulated for soybean, for each point of the MP2 pluviometry grid. Theoretical sowing dates: November 15, 2016, December 15, 2016, and January 15, 2017. Grouping results of the FAO – Agroecological Zone, MONICA, and DSSAT models.

	Nov 15, 2016			Dec 15, 2016			Jan 15, 2017		
Point	AC (mm)	PA (Kg ha ⁻¹)	Yg (%)	AC. (mm)	PA (Kg ha ⁻¹)	Yg (%)	AC (mm)	PA (Kg ha ⁻¹)	Yg (%)
P1	701.4	4275.3	33.7	655.2	3712.3	37.9	524.3	2449.6	49.9
P2	742.5	4467.8	30.7	707.7	4116.3	31.2	592.1	2765.3	43.7
P3	695.7	4266.7	33.8	646.7	3673.2	38.3	516.2	2424.0	50.5
P4	673.2	4249.3	34.0	621.9	3624.9	39.1	500.9	2327.5	52.3
P5	698.3	4220.4	34.4	645.7	3606.4	39.4	529.9	2386.7	51.4
P6	702.7	4215.5	34.5	643.6	3583.4	39.7	521.5	2321.0	52.7
P7	688.7	4239.3	34.1	637.9	3544.2	40.4	517.2	2291.2	53.3
P8	699.2	4210.8	34.6	645.4	3558.7	40.1	526.8	2328.8	52.5
P9	651.1	4077.8	36.5	598.7	3392.4	42.9	483.8	2234.4	54.2
Mean	694.8	4247.0	34.0	644.8	3645.8	38.8	523.6	2392.0	51.2
SD	24.5	101.0	1.5	29.1	198.3	3.2	29.5	154.9	3.1
CV	3.5	2.4	4.4	4.5	5.4	8.2	5.6	6.5	6.1

SD is the standard variation; CV is the coefficient of variation (%).

Likewise, simulations based on MP2 data (Table 2) did not include spatial variability in air temperature and global solar radiation (Fig. 5). The grouping of the models estimated potential yield of 6,366.0 kg ha⁻¹, 5,964.7 kg ha⁻¹, and 4,942.0 kg ha⁻¹ respectively for the series started on November 15, 2016, December 15, 2016, and January 15, 2017. The PP results for the same sowing dates, as a function of air temperature and global solar radiation data (Figs. 5), were similar, and again corroborated by the results described by Battisti (2016) and Silva (2018).

The average attainable yield (PA) of the three models (Table 2) once again revealed how a meteorological element can be a source of yield variability within production areas (O'Neal et al., 2002). The mean PA for

the first series (sowing on November 15, 2016) was 4,247.0 kg ha⁻¹, with a standard deviation of 101.0 kg ha⁻¹. For the other two series analyzed, the results showed the same trend, with a PA of 3,645.8 (± 198.3) kg ha⁻¹ for the second and 2,392.0 (± 154.9) kg ha⁻¹ for the third series (Table 2).

The simulated yield losses (Yg) as a function of water availability for MP2 (Table 2) were higher than those determined for MP1 (Table 1) for all sowing dates. For the first sowing date (November 15) the MP2 grid loss was 34%, increasing to 38.8% and 51.2% for simulated sowing dates on December 15, 2016, and January 15, 2017, respectively (Table 2). Despite reductions in cycle length with sowing delay, the reduction in accumulated precipitation, which extrapolated the reductions in cycle length and, logically, the temporal distribution over the production cycle (Fig. 3), were responsible for the greatest yield losses registered in the MP2.

Analyzing the attainable yield data from each sampling point of the two grids for all three-production series analyzed (Tables 1 and 2), it is reiterated that there is no direct relationship between the accumulated precipitation and the attainable yield of a production cycle of soybean crop (Fig. 6). Based on the approach proposed by van Ittersun et al. (2013), from a “boundary layer”, elucidate the yield differences (Ya) due to the temporal distribution of rainfall over oilseed cultivation.

Purcell and Specht (2004) point out that not only the total amount but also the distribution of water supply during the growing season (Figs. 2 and 3) can explain the differences in soybean yield. This interpretation is extremely important in the analysis of the relationship between yield and the management of soybean production areas (Grassini et al. 2015; Zanon et al. 2016), especially in areas conducted with precision agriculture, where it is important to understand yield variability.

The spatial variability of yield associated with precipitation (Tables 1 and 2, Fig. 6) is jointly analyzed with management, soil, topography, pests, and diseases (Paz et al. 1998; Kravchenko and Bullock 2002; Kravchenko et al. 2005; Verhulst et al. 2009) has shown that in well-managed areas, water availability is the main cause of yield loss.

4. Conclusions

The objective of this article was to analyze the uncertainties regarding the homogeneity of precipitation in hypothetical soybean production areas, with 1,000.0 ha and 36.0 ha. The motivation for the work was to analyze how the meteorological factor can be related to yield variability in production areas. Therefore, data from two experiments were used, both with nine rain gauges within an area of 1,000.0 ha (MP1) and 36.0 ha (MP2). The study determined the variability of precipitation and the possible effect of this variability on soybean yield, based on simulations, for three sowing dates. The precipitation data described the variability between the measurement points, as well as the differences between the different simulated sowing dates. Soybean production was simulated by three models, using the average of the set. The effect of rainfall variability on attainable yield was determined from standard deviation and CV. From the MP1 data, a standard deviation of up to 160 kg ha⁻¹ was observed for attainable yield.

For MP2, the standard deviation to the average attainable yield reached 198.3 kg ha⁻¹, solely due to precipitation variability. The results also showed the influence of the temporal variability of precipitation on the phenology of the soybean crop, with greater or lesser influence depending on the susceptibility of the crop to water stress.

Declarations

Funding

This work was supported by *The São Paulo Research Foundation (FAPESP)*, Grant Number: 2015/14497-0.

Competing Interest

The authors declare that they have no known competing financial interests or personal relationships that could have appeared to influence the work reported in this paper.

Author Contributions

Felipe Gustavo Pilau was responsible for the study conception and design. Material preparation, data collection and analysis were performed by Felipe Gustavo Pilau, Thais Letícia dos Santos, Rafael Battisti, Klaus Reichardt and Ivo Zution Gonçalves. The first draft of the manuscript was written by Felipe Gustavo Pilau and Thais Letícia dos Santos, and all authors commented on previous versions of the manuscript. All authors read and approved the final manuscript.

Data availability

Data will be made available on request.

References

1. Almeida CT, Oliveira-Júnior JF, Delgado RC, Cubo P, Ramos MC (2016) Spatiotemporal rainfall and temperature trends throughout the Brazilian Legal Amazon, 1973–2013. *Int. J. Clim.* 37:2013–2026. DOI: 10.1002/joc.4831
2. Alvares CA, Stape JL, Sentelhas PC, Gonçalves JL de M, Sparovek G (2013) Köppen's climate classification map for Brazil. *Meteorologische Zeitschrift* 22(6):711–728. DOI: 10.1127/0941-2948/2013/0507
3. Amado T, Pontelli CB, Santi AL, Viana J, Sulzbach LA de S (2007) Spatial and temporal variability of grain yield under no-tillage cropping system. *Pesquisa Agropecuária Brasileira* 42(8):1101–1110. <https://doi.org/10.1590/S0100-204X2007000800006>.
4. Ashouri H, Hsu K, Sorooshian S, Braithwaite DK, Knapp KR, Cecil LD, Nelson BR, Prat OP (2015) PERSIANN-CDR: Daily precipitation climate data record from multisatellite observations for

- hydrological and climate studies. *American Meteorological Society* 96:69–83.
<https://doi.org/10.1175/BAMS-D-13-00068.1>
5. Asseng S, Ewert F, Rosenzweig C, Jones JW, Hatfield JL, Ruane AC, Boote KJ, Thorburn PJ, Rötter RP, Cammarano D, Brisson N, Basso B, Martre P, Aggarwal PK, Angulo C, Bertuzzi P, Biernath C, Challinor AJ, Doltra J, Gayler S, Goldberg R, Grant R, Heng L, Hooker J, Hunt LA, Ingwersen J, Izaurralde RC, Kersebaum KC, Müller C, Naresh Kumar S, Nendel C, O’Leary G, Olesen JE, Osborne TM, Palosuo T, Priesack E, Ripoche D, Semenov MA, Shcherbak I, Steduto P, Stöckle C, Stratonovitch P, Streck T, Supit I, Tao F, Travasso M, Waha K, Wallach D, White JW, Williams JR, Wolf J (2013) Uncertainty in simulating wheat yields under climate change. *Nature Climate Change*, 3(9):827–832. DOI: 10.1038/NCLIMATE1916
 6. Battisti R (2016) Calibration, uncertainties and use of soybean crop simulation models for evaluating strategies to mitigate the effects of climate change in Southern Brasil. Thesis, Escola Superior de Agricultura “Luiz de Queiroz”, Universidade de São Paulo.
 7. Battisti R, Sentelhas PC, Boote KJ (2017) Inter-comparison of performance of soybean crop simulation models and their ensemble in southern Brazil. *Field Crops Research* 200:28–37. <https://doi.org/10.1016/j.fcr.2016.10.004>
 8. Battisti R, Sentelhas PC, Pilau FG, Wollmann CA (2013) Eficiência climática para as culturas da soja e do trigo no estado do Rio Grande do Sul em diferentes datas de semeadura. *Cienc. Rural* 43(3):390–396. <https://doi.org/10.1590/S0103-84782013000300003>.
 9. Bega RM, Vieira SR, Maria IC de, Dechen SNF, Castro OM de (2005) Variabilidade espacial das precipitações pluviométricas diárias em uma estação experimental, em Pindorama, SP. *Bragantia* 64(1):149–156. <https://doi.org/10.1590/S0006-87052005000100016>.
 10. Boote KJ, Jones JW, Batchelor WD, Nafziger ED, Myers O (2003) Genetic Coefficients in the CROPGRO–Soybean Model. *Agron. J.* 95:32–51. <https://doi.org/10.2134/agronj2003.3200>
 11. Boote KJ, Jones JW, Hoogenboom G (1998) Simulation of crop growth: CROPGRO model. In: Peart, R.M., & Shoup, W.D. (ed). *Agricultural Systems Modeling and Simulation*, 1st edn. CRC Press. <https://doi.org/10.1201/9781482269765>
 12. Bottega EL, Queiroz DM de, Pinto F de A de C, Souza CMA de, Valente DSM (2017) Precision agriculture applied to soybean: Part I - delineation of management zones. *Australian Journal of Crop Science* 11(5):573–579. DOI: 10.21475/ajcs.17.11.05.p381
 13. Camargo MBP, Brunini O, Junior MJP, Bardin L (2005) Variabilidade espacial e temporal de dados termopluiométricos diários da rede de estações agrometeorológicas do Instituto Agrônômico (IAC). *Bragantia* 64(3):473–483. <https://doi.org/10.1590/S0006-87052005000300018>
 14. Camargo MBP, Hubbard KG (1999) Spatial and temporal variability of daily weather variables in sub-humid and semi-arid areas of the united states high plains. *Agricultural and Forest Meteorology* 93(2):141–148. [https://doi.org/10.1016/S0168-1923\(98\)00122-1](https://doi.org/10.1016/S0168-1923(98)00122-1)
 15. Chierice RAF, Landim PMB (2014) Variabilidade espacial e temporal de precipitação pluviométrica na bacia hidrográfica do rio Mogi Guaçu. *Revista Geociências* 33(1):157–171.

16. Dalchiavon FC, Rodrigues AR, de Lima ES, Lovera LH, Montanari R (2017) Variabilidade espacial de atributos químicos do solo cultivado com soja sob plantio direto. *Revista de Ciências Agroveterinárias* 16(2):144–154. DOI: 10.5965/223811711622017144
17. Doorenbos J, Kassam AH (1979) Yield response to water. FAO irrigation and drainage paper No. 33. FAO, Rome, Italy.
18. Estévez J, Gavilán P, Giráldez JV (2011) Guidelines on validation procedures for meteorological data from automatic weather stations. *Journal of Hydrology* 402(1–2):144–154. <https://doi.org/10.1016/j.jhydrol.2011.02.031>
19. Faraco MA, Uribe-Opazo MA, Silva EAA, Johann JA, Borssoi JA (2008) Seleção de modelos de variabilidade espacial para elaboração de mapas temáticos de atributos físicos do solo e produtividade da soja. *Revista Brasileira de Ciências do Solo* 32:463–476. <https://doi.org/10.1590/S0100-06832008000200001>
20. Farias JRB, Nepomuceno AL, Neumaier N (2007) *Ecofisiologia da soja*. Londrina Embrapa (Circular Técnica 48).
21. Funk C, Peterson P, Landsfeld M, Pedreros D, Verdin J, Shukla S, Husak G, Rowland J, Harrison L, Hoell A, Michaelsen J (2015) The climate hazards infrared precipitation with stations - a new environmental record for monitoring extremes. *Scientific Data* 2:1–21 DOI: 10.1038/sdata.2015.66.
22. Gires A, Tchiguirinskaia I, Schertzer D, Schellart A, Berne A, Lovejoy S (2014) Influence of small scale rainfall variability on standard comparison tools between radar and rain gauge data. *Atmospheric Research* 138:125–138. <https://doi.org/10.1016/j.atmosres.2013.11.008>
23. Gleason ML, Duttweiler KB, Batzer JC, Taylor SE, Sentelhas PC, Monteiro JEBA, Gillespie TJ (2008) Obtaining weather data for input to crop disease-warning systems: leaf wetness duration as a case study. *Sci. Agric.* 65:76–87. <https://doi.org/10.1590/S0103-90162008000700013>
24. Graef F, Haigis J (2001) Spatial and temporal rainfall variability in the Sahel and its effects on farmers' management strategies. *Journal of Arid Environments* 48(2):221–231. [doi:10.1006/jare.2000.0747](https://doi.org/10.1006/jare.2000.0747)
25. Grassini P, Torrión JA, Yang HS, Rees J, Andersen D, Cassman KG, Specht JE (2015) Soybean yield gaps and water productivity in the Western U.S. Corn Belt. *Field Crops Research* 179:150–163. <http://dx.doi.org/10.1016/j.fcr.2015.04.015>
26. Huffman GJ, Adler RF, Bolvin DT, Gu G, Nelkin EJ, Bowman KP, Hong Y, Stocker EF, Wolff DB (2007) The TRMM Multisatellite Precipitation Analysis (TMPA): Quasi-Global, Multiyear, Combined-Sensor Precipitation Estimates at Fine Scales. *Journal of Hydrometeorology* 8(1):38–55. <https://doi.org/10.1175/JHM560.1>
27. Huffman GJ, Bolvin DT, Braithwaite D, Hsu K, Joyce R, Kidd C, Nelkin EJ, Sorooshian S, Tan J, Xie P (2019) NASA Global Precipitation Measurement (GPM) Integrated Multi-satellite Retrievals for GPM (IMERG). In: Algorithm Theoretical Basis Document (ATBD). Available in: https://docserver.gesdisc.eosdis.nasa.gov/public/project/GPM/IMERG_ATBD_V06.pdf

28. Jayaraman PP, Yavari A, Georgakopoulos D, Morshed A, Zaslavsky A (2016) Internet of things platform for smart farming: experiences and lessons learnt. *Sensors* 16:1884; doi:10.3390/s16111884
29. Jensen NE, Pedersen L (2005) Spatial variability of rainfall: variations within a single radar pixel. *Atmospheric Research* 77(1–4):269–277. <https://doi.org/10.1016/j.atmosres.2004.10.029>
30. Jones JW, Hoogenboom G, Porter CH, Boote KJ, Batchelor WD, Hunt LA, Wilkens PW, Singh U, Gijsman AJ, Ritchie JT (2003) The DSSAT cropping system model. *Europ. J. Agronomy* 18:235–265. DOI: 10.1016/S1161-0301(02)00107-7
31. Keswani B, Mohapatra AG, Mohanty A, Khanna A, Rodrigues JJPC, Gupta D, Albuquerque VHC de M (2019) Adapting weather conditions based IoT enabled smart irrigation technique in precision agriculture mechanisms. *Neural Comput & Applic.* 31:277–292. <https://doi.org/10.1007/s00521-018-3737-1>
32. Krajewski WF, Ciach GJ, Habib E (2003) An analysis of small-scale rainfall variability in different climatic regimes. *Hydrological Sciences Journal* 48(2):151–162. <https://doi.org/10.1623/hysj.48.2.151.44694>
33. Kravchenko AN, Bullock DG (2002) Spatial variability of soybean quality data as a function of field topography: I. spatial data analysis. *Crop Sci.* 42(3):804–815. <https://doi.org/10.2135/cropsci2002.8040>
34. Kravchenko AN, Robertson GP, Thelen KD, Harwood RR (2005) Management, topographical, and weather effects on spatial variability of crop grain yields. *Agron. J.* 97:514–523. DOI: 10.2134/agronj2005.0514
35. Lamb DW, Brown RB (2001) Remote-sensing and mapping of weeds in crops. *J. agric. Engng Res.* 78(2):117–125. <https://doi.org/10.1006/jaer.2000.0630>
36. Lenzi G, Nanni S, Salsi A (1990) Agricultural use of weather radar data in Emilia-Romagna Italy. In: Collier, C.G., Chapuis, M. (ed) *Weather radar networking*. Springer, Dordrecht. https://doi.org/10.1007/978-94-009-0551-1_57
37. Lobell DB (2013) The use of satellite data for crop yield gap analysis. *Field Crops Research* 143:56–64. <https://doi.org/10.1016/j.fcr.2012.08.008>
38. Lobell DB, Thau D, Seifert C, Engle E, Little B (2015) A scalable satellite-based crop yield mapper. *Remote Sensing of Environment* 164:324–333. <https://doi.org/10.1016/j.rse.2015.04.021>
39. Martre P, Wallach D, Asseng S, Ewert F, Jones JW, Rötter RP, Boote KJ, Ruane AC, Thorburn PJ, Cammarano D, Hatfield JL, Rosenzweig C, Aggarwal PK, Angulo C, Basso B, Bertuzzi P, Biernath C, Brisson N, Challinor AJ, Doltra J, Gayler S, Goldberg R, Grant RF, Heng L, Hooker J, Hunt LA, Ingwersen J, Izaurralde RC, Kersebaum KC, Müller C, Kumar SN, Nendel C, O’leary G, Olesen JE, Osborne TM, Palosuo T, Priesack E, Ripoche D, Semenov MA, Shcherbak I, Steduto P, Stöckle CO, Stratonovitch P, Streck T, Supit I, Tao F, Travasso M, Waha K, White JW, Wolf J (2015) Multimodel ensembles of wheat growth: many models are better than one. *Global Change Biology* 21(2):911–925. doi: 10.1111/gcb.12768

40. Mashingia F, Mtalo F, Bruen M (2014) Validation of remotely sensed rainfall over major climatic regions in Northeast Tanzania. *Physics and Chemistry of the Earth* 67–69:55–63.
<https://doi.org/10.1016/j.pce.2013.09.013>
41. Mattioni NM, Schuch LOB, Villela FA (2011) Variabilidade espacial da produtividade e da qualidade das sementes de soja em um campo de produção. *Rev. bras. Sementes* 33(4):608–615.
<https://doi.org/10.1590/S0101-31222011000400002>
42. Mattioni NM, Schuch LOB, Villela FA, Zen HD, Mertz LM (2013) Fertilidade do solo na qualidade fisiológica de sementes de soja. *Revista Brasileira de Ciências Agrárias* 8(4):656–661.
DOI:10.5039/agraria.v8i4a3495
43. Mega T, Ushio T, Kubota T, Kachi M, Aonashi K, Shige S (2014) Gauge adjusted global satellite mapping of precipitation (GSMaP_Gauge). XXXIth URSI General Assembly and Scientific Symposium (URSI GASS), Beijing, China, pp. 1–4, doi: 10.1109/URSIGASS.2014.6929683.
44. Mesas-Carrascosa FJ, Santano DV, Meroño JE, Orden MS de la, García-Ferrer A (2015) Open source hardware to monitor environmental parameters in precision agriculture. *Biosystems Engineering* 137:73–83. <https://doi.org/10.1016/j.biosystemseng.2015.07.005>
45. Ministério da Agricultura, Pecuária e Abastecimento, MAPA (2018) Portarias de zoneamento agrícola de risco climático. Available in: <http://www.agricultura.gov.br/assuntos/riscos-seguro/risco-agropecuário/portarias/safra-vigente/rio-grande-do-sul>. Accessed: February, 15 2021
46. Monquero PA, Amaral LR, Binha DP, Silva PV, Silva AC, Martins FRA (2008) Mapas de infestação de plantas daninhas em diferentes sistemas de colheita da cana-de-açúcar. *Planta Daninha* 26(1):47–55. <http://dx.doi.org/10.1590/S0100-83582008000100005>.
47. Nendel C, Berg M, Kersebaum JC, Mirschel W, Specka X, Wegehenkel M, Wenkel KO, Wieland R (2011) The MONICA model: testing predictability for crop growth, soil moisture and nitrogen dynamics. *Ecological Modelling* 222:1614–1625. <https://doi.org/10.1016/j.ecolmodel.2011.02.018>
48. Oliveira RK (2018) Fluxos de CO₂, água e energia em áreas de renovação de canavial com cultivo de soja. Dissertation, Escola Superior de Agricultura “Luiz de Queiroz”, Universidade de São Paulo.
49. O'Neal MR, Frankenberger JR, Ess DR (2002) Use of CERES-Maize to study effect of spatial precipitation variability on yield. *Agricultural Systems* 73(2):205–225.
[https://doi.org/10.1016/S0308-521X\(01\)00095-6](https://doi.org/10.1016/S0308-521X(01)00095-6)
50. Paz JO, Batchelor WD, Colvin TS, Logsdon SD, Kaspar TC, Karlen DL (1998) Analysis of water stress effects causing spatial yield variability in soybeans. *Transactions of the ASAE* 41(5):1527–1534.
DOI: 10.13031/2013.17284
51. Pedersen L, Jensen NE, Christensen LE, Madsen H (2010) Quantification of the spatial variability of rainfall based on a dense network of rain gauges. *Atmospheric Research* 95(4):441–454.
<https://doi.org/10.1016/j.atmosres.2009.11.007>
52. Pierce FJ, Elliott TV (2008) Regional and on-farm wireless sensor networks for agricultural systems in Eastern Washington. *Computers and Electronics in Agriculture* 61:32–43.
<https://doi.org/10.1016/j.compag.2007.05.007>

53. Purcell LC, Specht JE (2004) Physiological traits for ameliorating drought stress. In: Soybeans: Improvement, production, and uses. (eds R.M. Shibles, J.E. Harper, R.F. Wilson and R.C. Shoemaker). <https://doi.org/10.2134/agronmonogr16.3ed.c12>
54. Reichardt K, Angelocci LR, Bacchi OOS, Pilotto JE (1995) Daily rainfall variability at a local scale (1,000 ha), in Piracicaba, SP, Brazil, and its implications on soil water recharge. *Scientia Agricola* 52(1): 43–49. <https://doi.org/10.1590/S0103-90161995000100008>.
55. Robertson MJ, Carberry PS (1998) Simulating growth and development of soybean in APSIM. Proceedings 10th Australian Soybean Conference, Brisbane 15–17 September, 130–136.
56. Schilling W (1991) Rainfall data for urban hydrology: what do we need? *Atmospheric Research* 27(1–3):5–21. [https://doi.org/10.1016/0169-8095\(91\)90003-F](https://doi.org/10.1016/0169-8095(91)90003-F)
57. Siciliano WC, Bastos GP, Oliveira IT de, Silva GN da, Obraczka M, Ohnuma Jr AA (2018) Variabilidade espacial e temporal da precipitação pluvial no município do Rio de Janeiro. *Revista Internacional de Ciências* 8(2):221–233. DOI: 10.12957/ric.2018.33811
58. Silva EHF da (2018) Simulação de cenários agrícolas futuros para a cultura da soja no Brasil com base em projeções de mudanças climáticas. Dissertation, Escola Superior de Agricultura “Luiz de Queiroz”, Universidade de São Paulo.
59. Souza TS de, Nascimento P dos S (2020) Análise da variabilidade espacial e temporal da precipitação pluviométrica na região hidrográfica do Recôncavo Sul (BA). *Revista Brasileira de Climatologia* 27:1–18. DOI: <http://dx.doi.org/10.5380/abclima.v27i0.68353>
60. Stol PT (1972) The relative efficiency of the density of rain-gage networks. *Journal of Hydrology* 15(3):193–208. [https://doi.org/10.1016/0022-1694\(72\)90013-3](https://doi.org/10.1016/0022-1694(72)90013-3)
61. Tokay A, Roche RJ, Bashor PG (2014) An experimental study of spatial variability of rainfall. *Journal of Hydrometeorology* 15(2):801–812. <https://doi.org/10.1175/JHM-D-13-031.1>
62. van Genuchten MT (1980) A closed form equation for predicting the hydraulic conductivity of unsaturated soils. *Soil Science Society of America Journal* 44(5):892–898. <https://doi.org/10.2136/sssaj1980.03615995004400050002x>
63. van Ittersum MK, Cassman KG, Grassini P, Wolf J, Tittone P, Hochman Z (2013) Yield gap analysis with local to global relevance - a review. *Field Crops Research* 143:4–17. <https://doi.org/10.1016/j.fcr.2012.09.009>
64. Venäläinen A, Heikinheimo MA (2002) Meteorological data for agricultural applications. *Physics and Chemistry of the Earth* 27:1045–1050. [https://doi.org/10.1016/S1474-7065\(02\)00140-7](https://doi.org/10.1016/S1474-7065(02)00140-7)
65. Verhulst N, Govaerts B, Sayre KD, Deckers J, François IM, Dendooven L (2009) Using NDVI and soil quality analysis to assess influence of agronomic management on within-plot spatial variability and factors limiting production. *Plant and Soil* 317:41–59. DOI 10.1007/s11104-008-9787-x
66. Zanon AJ, Streck NA, Grassini P (2016) Climate and management factors influence soybean yield potential in a subtropical environment. *Agronomy Journal* 108(4):1447–1454. <https://doi.org/10.2134/agronj2015.0535>

Figures

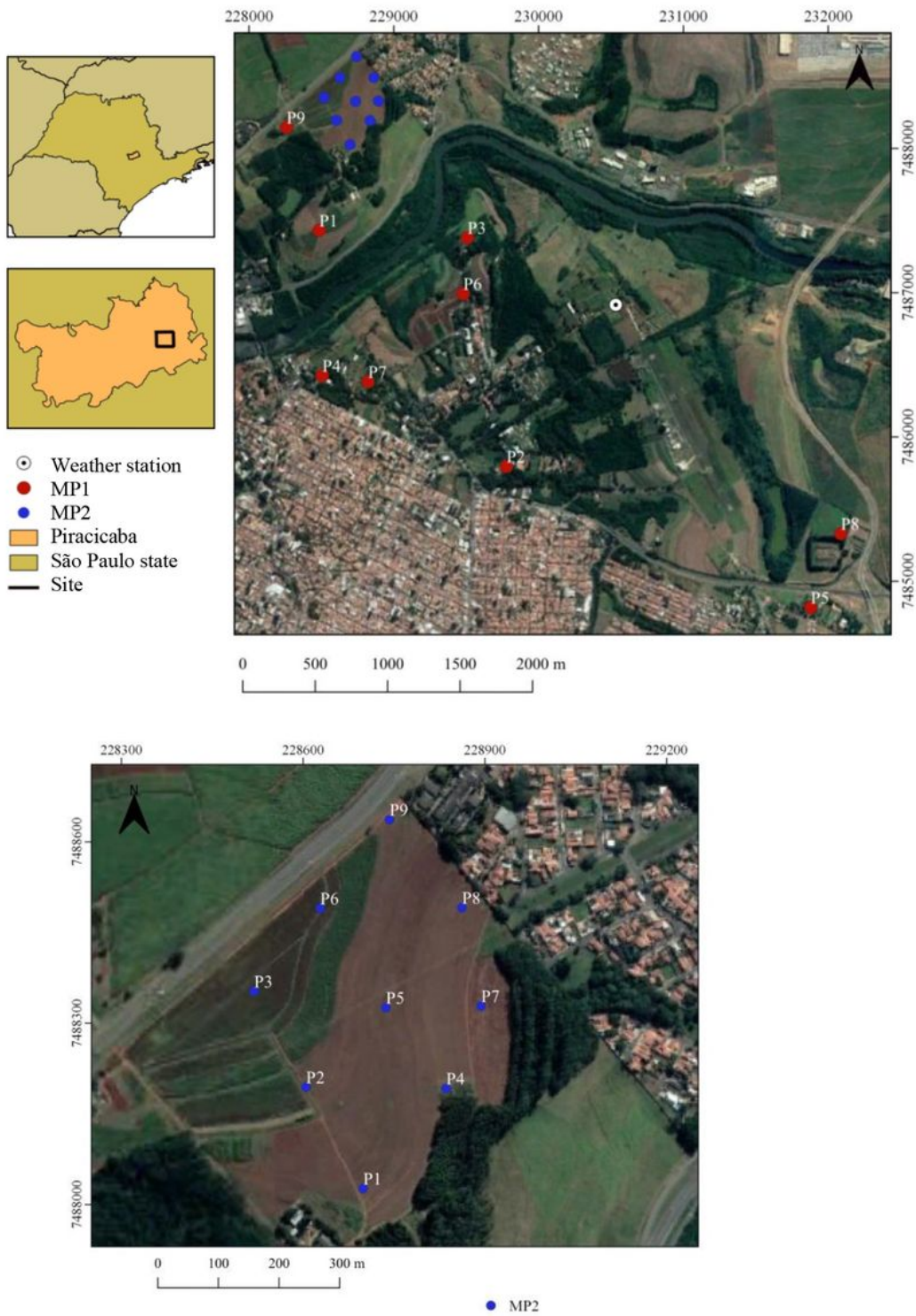


Figure 1

Location of the study area in Piracicaba, state of São Paulo, Brazil, and positioning of the two pluviometry grids (MP1 and MP2) in the ESALQ/USP area.

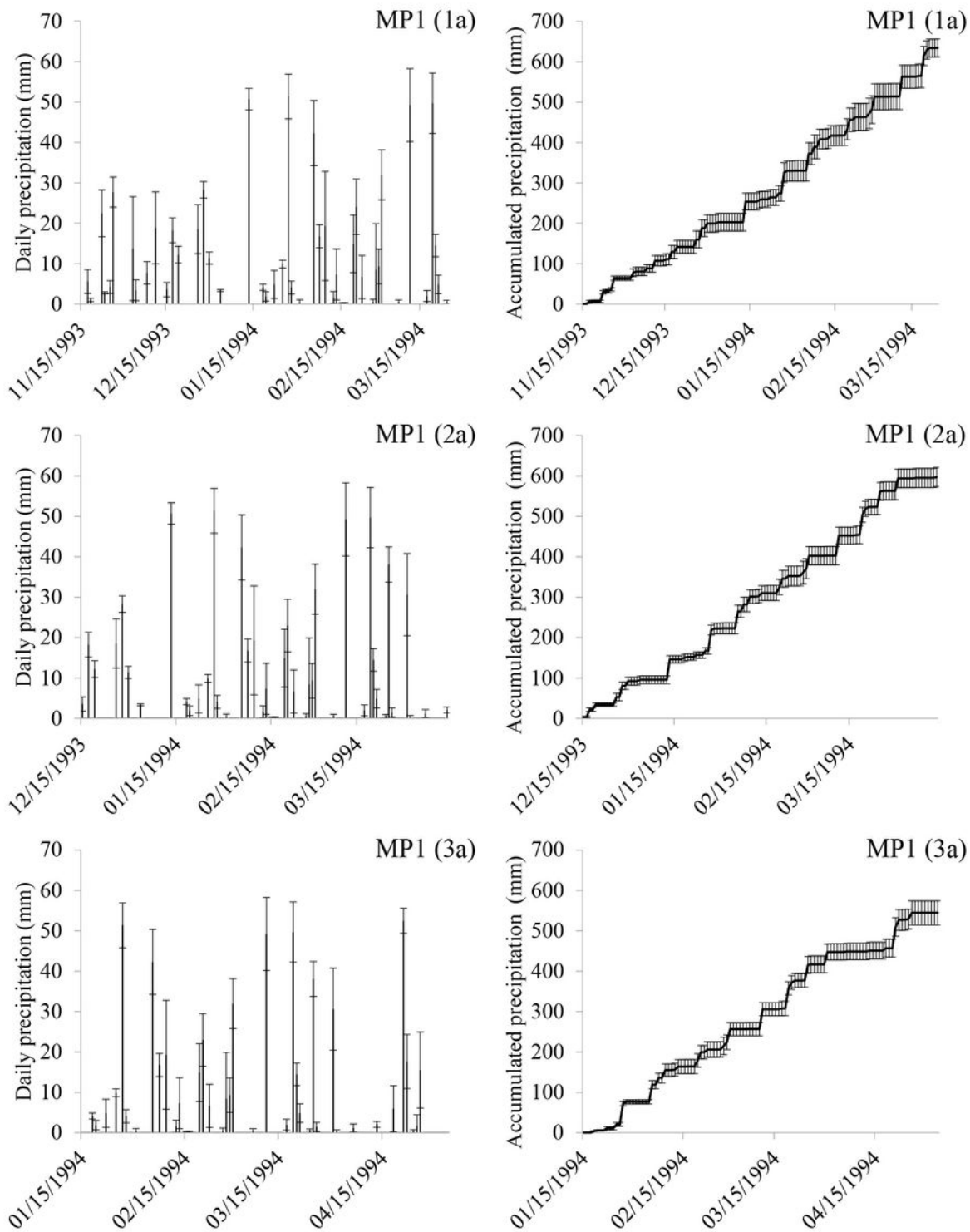


Figure 2

Daily and accumulated precipitation during the three series of the MP1 grid, with 130 [MP1(1a)], 120 [MP1(2a)], and 110 [MP1(3a)] days, respectively measured from 11/15/1993, 12/15/1993 and 01/15/1994, coinciding with the soybean production season in Piracicaba (SP).

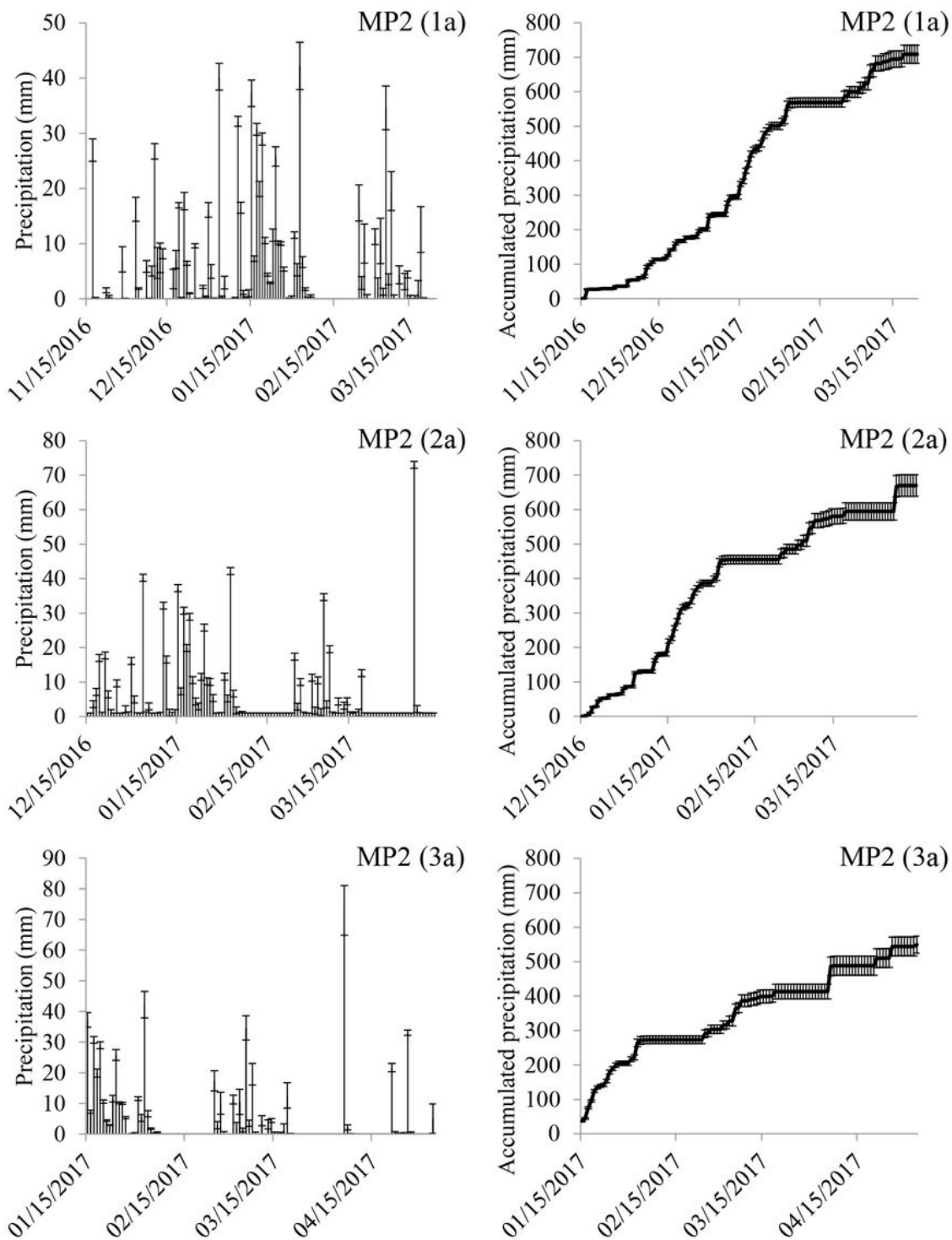


Figure 3

Daily and accumulated precipitation during the three series of the MP2 grid, with 130 [MP2(1a)], 120 [MP2(2a)], and 110 [MP2(3a)] days, respectively measured from 11/15/ 2016, 12/15/2016 and 15/01/2017, coinciding with the soybean production seasons in Piracicaba (SP).

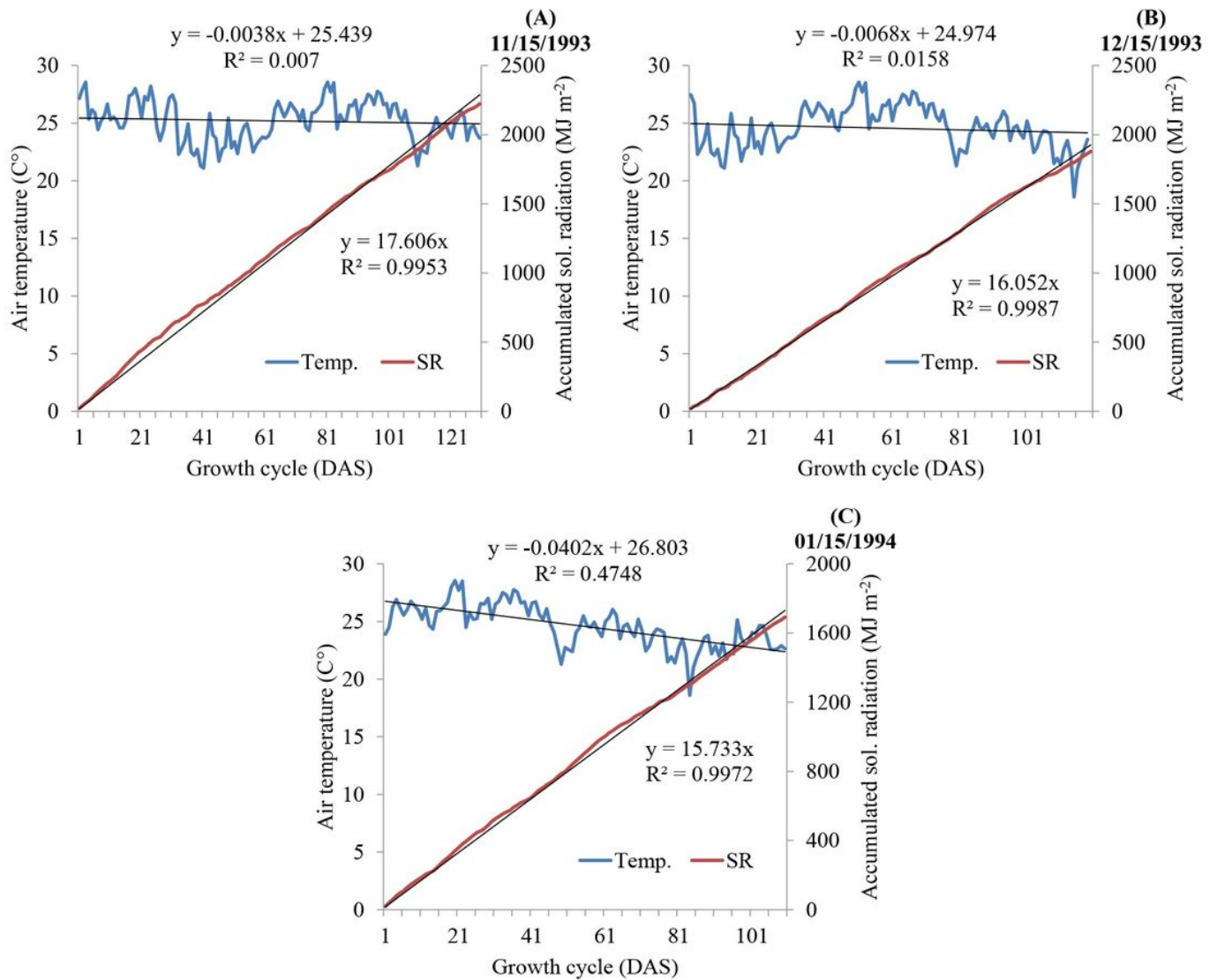


Figure 4

Average air temperature and global solar radiation accumulated over the series related to soybean production cycles of MP1, measured from 11/15/1993 (A), 12/15/1993 (B), and 01/15/1994 (C).

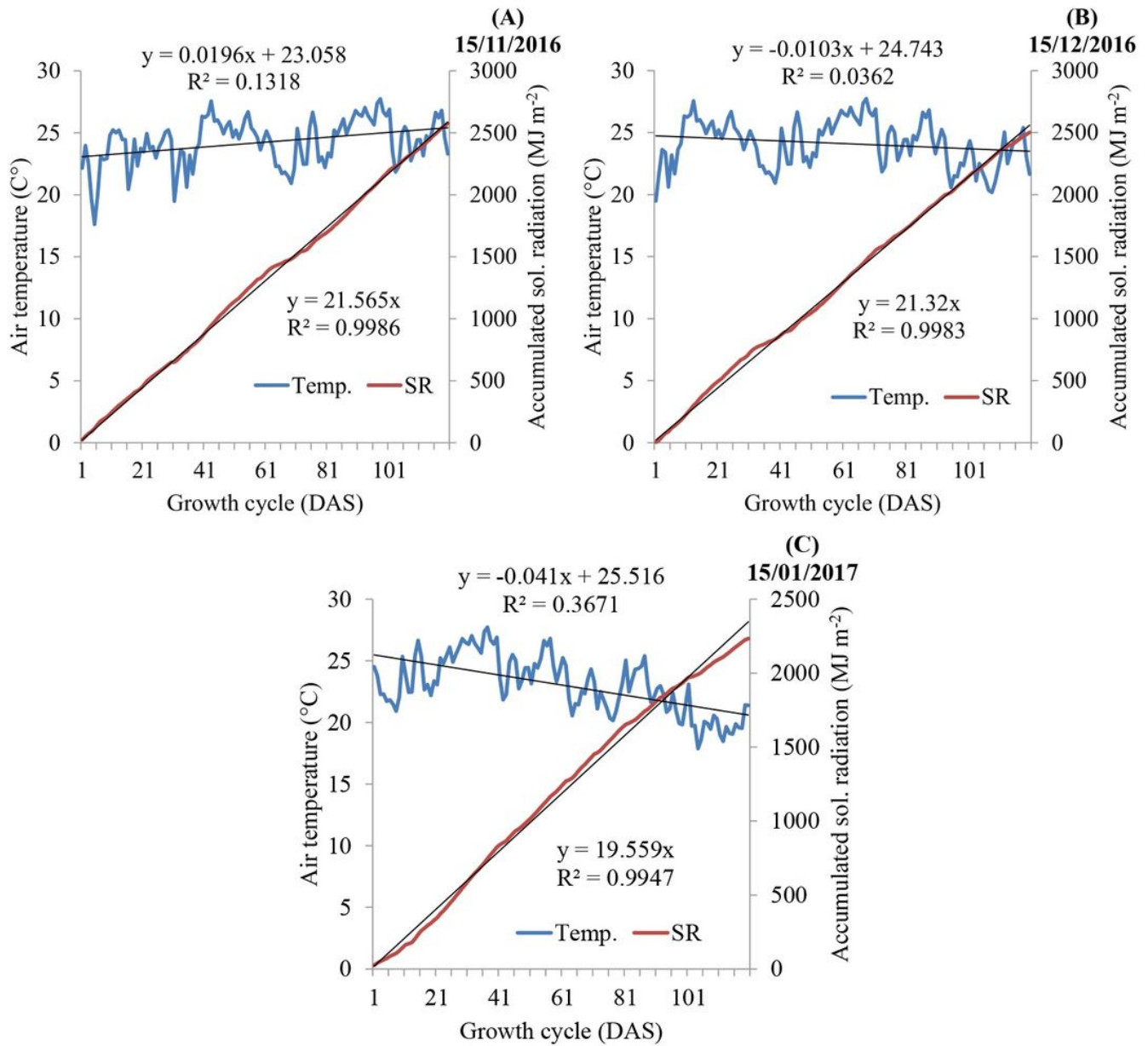


Figure 5

Average air temperature and global solar radiation accumulated over the series related to soybean production cycles of MP2, measured from 11/15/2016 (A), 12/15/2016 (B), and 01/ 15/2017 (C).

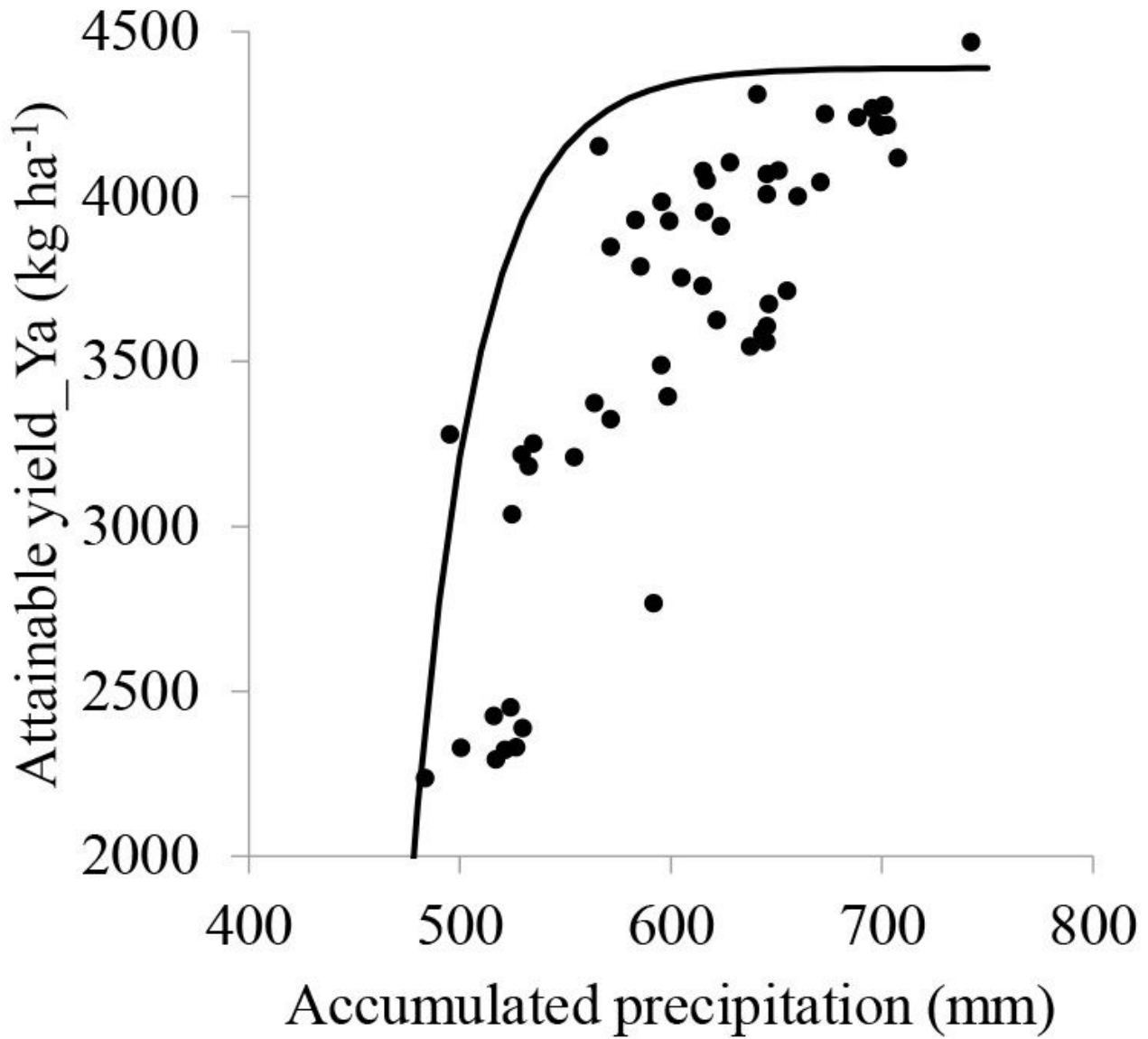


Figure 6

Correlation between attainable soybean yield (Y_a) and accumulated precipitation in the cropping cycle, referring to the simulations of each sampling point in the MP1 and MP2 grids for the three analyzed soybean production series. The solid line represents the “boundary layer” for attainable yield (Y_a).